

Research Article

Solid Solutions of $\text{LiCo}_{1-x}\text{Ni}_x\text{O}_2$ ($x = 0, 0.1, \dots, 0.9$) Obtained via a Combustion Synthesis Route and Their Electrochemical Characteristics

Kelimah Elong,^{1,2} Norlida Kamarulzaman,^{1,2} Roshidah Rusdi,^{1,2}
Nurhanna Badar,^{1,2} and Mohd Hilmi Jaafar³

¹ Centre for Nanomaterials Research, Institute of Science, Level 3 Block C, Universiti Teknologi MARA, 40450 Shah Alam, Selangor, Malaysia

² Faculty of Applied Sciences, Universiti Teknologi MARA, 40450 Shah Alam, Selangor, Malaysia

³ Institute of Graduate Studies, Universiti Malaya, 50603 Kuala Lumpur, Malaysia

Correspondence should be addressed to Norlida Kamarulzaman; norlyk@salam.uitm.edu.my

Received 2 December 2012; Accepted 19 December 2012

Academic Editors: S. Bud'ko and R. Rossmannith

Copyright © 2013 Kelimah Elong et al. This is an open access article distributed under the Creative Commons Attribution License, which permits unrestricted use, distribution, and reproduction in any medium, provided the original work is properly cited.

Pure, single-phase and layered $\text{LiCo}_{1-x}\text{Ni}_x\text{O}_2$ materials with good cation ordering are not easy to synthesize. In this work, solid solutions of $\text{LiCo}_{1-x}\text{Ni}_x\text{O}_2$ ($x = 0, 0.1, \dots, 0.9$) are synthesized using a self-propagating combustion route and characterized. All the materials are observed to be phase pure giving materials of hexagonal crystal system with $R\bar{3}m$ space group. The RIR and R factor values of stoichiometries of $\text{LiCo}_{1-x}\text{Ni}_x\text{O}_2$ ($x = 0.1, 0.2, 0.3, 0.4$, and 0.5) show good cation ordering. Their electrochemical properties are investigated by a series of charge-discharge cycling in the voltage range of 3.0 to 4.3 V. It is found that some of the stoichiometries exhibit specific capacities comparable or better than those of LiCoO_2 , but the voltage plateau is slightly more slopping than that for the LiCoO_2 reference material.

1. Introduction

Layered oxides are more advantageous over those of the spinels due to their higher theoretical specific capacities which are about double those of the spinels. The present commercial cathode material, LiCoO_2 , suffers from three major restrictions which are toxicity, cost, and scarcity. Therefore, it is logical to produce materials with less Co content [1] for commercial applications. LiNiO_2 has the advantage of being cheaper, but it is more difficult to synthesize and does not cycle well [1, 2]. It is thermodynamically as well as electrochemically unstable [3]. Thus, it is unsuitable for use in commercial Li-ion batteries. Cobalt substitution in LiNiO_2 is, however, more stable than its pure form [1]. $\text{LiCo}_{1-x}\text{Ni}_x\text{O}_2$ can be a potential commercial cathode if a relatively simple synthesis method yielding pure single-phase compounds is found.

Many groups of researchers [4–8] have attempted to synthesize some stoichiometries of $\text{LiCo}_{1-x}\text{Ni}_x\text{O}_2$, but their XRD results show the presence of impurities. Others such as

Xie et al. [9] and Lu and Wang [10] have produced hexagonal structure but with poor cation ordering with high (104) peaks relative to the (003) peak.

We present here a simple self-propagating combustion synthesis which produces pure, single-phase, and layered hexagonal-structured materials for the whole range of solid solutions of $\text{LiCo}_{1-x}\text{Ni}_x\text{O}_2$ ($x = 0, 0.1, \dots, 0.9$) with relatively good cation ordering especially for materials with $x \leq 0.4$ stoichiometries. Electrochemical behaviour of the materials was investigated, and it was found that some stoichiometries show comparable performance to LiCoO_2 reference material.

2. Experimental

$\text{LiCo}_{1-x}\text{Ni}_x\text{O}_2$ ($x = 0, 0.1, \dots, 0.9$) materials were synthesized using a self-propagating combustion method [11]. For the synthesis, lithium nitrate (LiNO_3 , Fluka), cobalt (II) nitrate hexahydrate ($\text{Co}(\text{NO}_3)_2 \cdot 6\text{H}_2\text{O}$, Aldrich), and nickel (II) nitrate ($\text{Ni}(\text{NO}_3)_2 \cdot \text{H}_2\text{O}$, Fluka) were used as starting materials. Nine Ni-substituted samples of $\text{LiCo}_{1-x}\text{Ni}_x\text{O}_2$

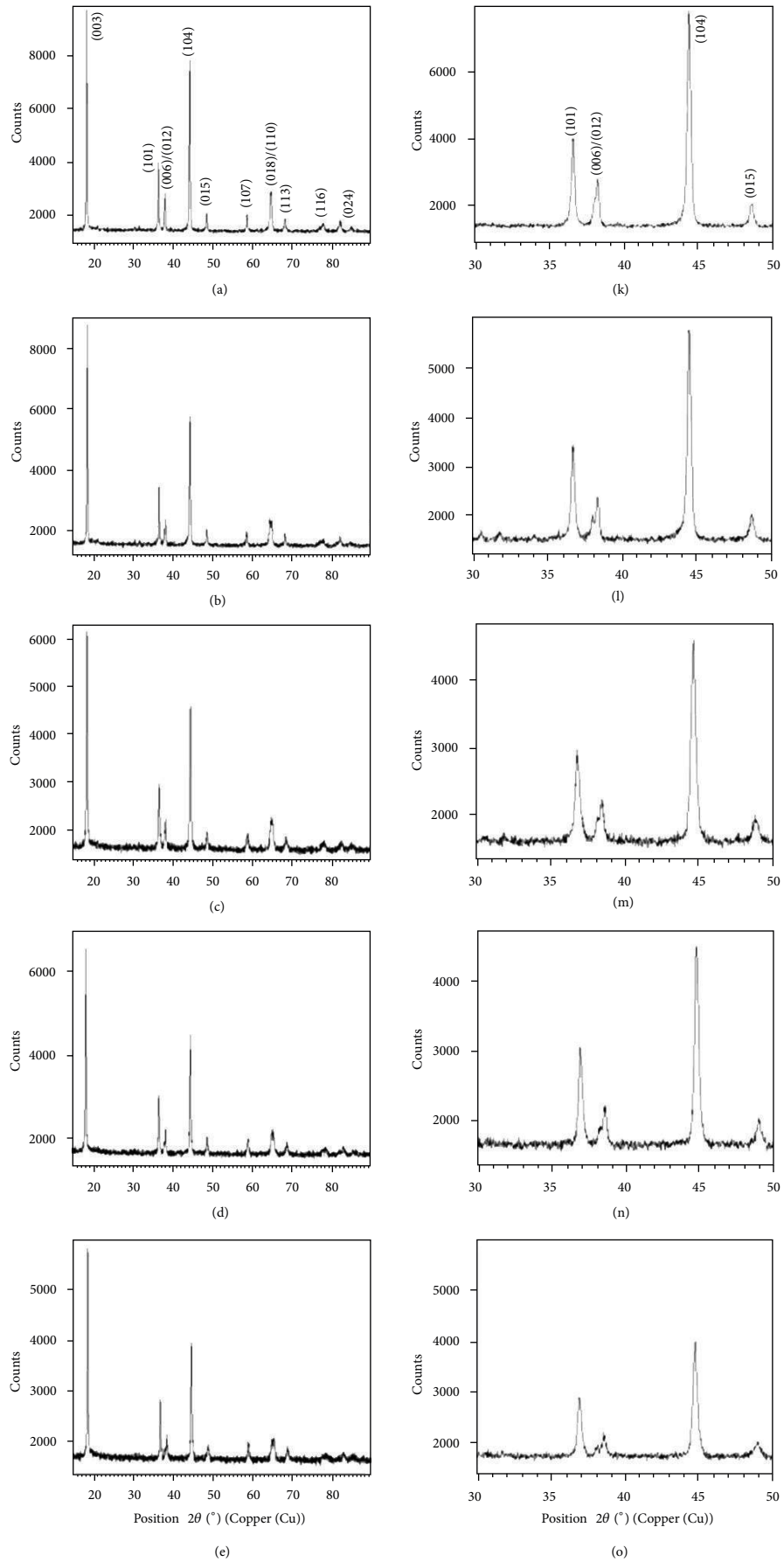


FIGURE 1: Continued.

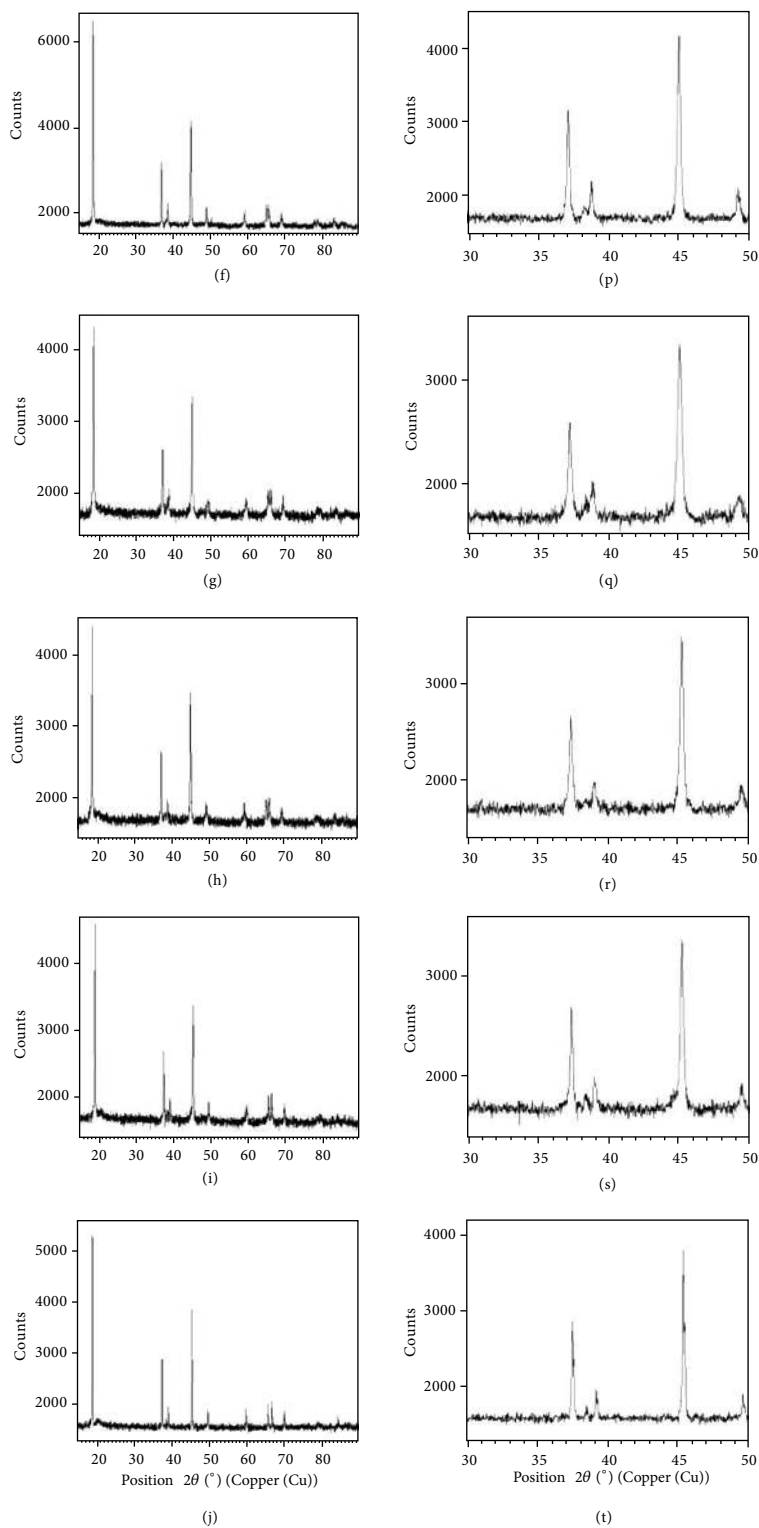


FIGURE 1: XRD patterns of (a) $\text{LiCo}_{0.1}\text{Ni}_{0.9}\text{O}_2$, (b) $\text{LiCo}_{0.2}\text{Ni}_{0.8}\text{O}_2$, (c) $\text{LiCo}_{0.3}\text{Ni}_{0.7}\text{O}_2$, (d) $\text{LiCo}_{0.4}\text{Ni}_{0.6}\text{O}_2$, (e) $\text{LiNi}_{0.5}\text{Co}_{0.5}\text{O}_2$, (f) $\text{LiCo}_{0.6}\text{Ni}_{0.4}\text{O}_2$, (g) $\text{LiCo}_{0.7}\text{Ni}_{0.3}\text{O}_2$, (h) $\text{LiCo}_{0.8}\text{Ni}_{0.2}\text{O}_2$, (i) $\text{LiCo}_{0.9}\text{Ni}_{0.1}\text{O}_2$, and (j) LiCoO_2 and enlargement of the XRD patterns at 30° and 50° for (k) to (t) materials.

($x = 0.1$ to 0.9) were prepared, and LiCoO_2 reference material was also prepared using the same synthesis route for a fair comparison. The starting materials were first dissolved in deionised water obtained from an ultrapure deionizing water system (TKA LabTower EDI: 15–10 M Ω cm) whereby a combusant, citric acid, was added according to stoichiometry. The mixture was stirred until homogeneous and slow heated until it reached its ignition conditions whereby combustion occurs. The combustion reaction is very fast and is over in a few seconds. The precursors obtained were annealed at 700°C for 24 h. The final products were grinded until fine and characterized.

Characterizations of the materials were done using X-ray diffraction (XRD) with Cu K_α radiation to identify the crystalline phase and purity of the materials. The XRD data was acquired with a PANalytical Xpert Pro powder diffraction equipment at room temperature and measured using the Bragg-Brentano optical configuration. The sample was prepared using the back loading method to minimise preferred orientation effects. The particle size and powder morphology of the synthesized materials were examined using scanning electron microscopy (SEM), using the JEOL JSM-7600F microscope.

The cathode was prepared using 80 wt% $\text{LiCo}_{1-x}\text{Ni}_x\text{O}_2$, 10 wt% polytetrafluoroethylene (PTFE) as binder, and 10 wt% Super P (a type of carbon) as an electronic conductor. The mixture was pressed onto metal grids, and the cathode was dried in an oven at 200°C for 24 h. The separator was a Celgard 2400 microporous polyethylene film, and lithium metal was used as anode. The electrolyte was 1.0 M lithium hexafluorophosphate, LiPF_6 in 1:1 volume ratio of ethylene carbonate (EC) and dimethyl carbonate (DMC) from Mitsubishi Chemical Corporation. The cells were assembled in a glove box (Unilab Mbraun) with oxygen and water content of less than 0.1 ppm. The cells were tested using a battery tester, the WonATech (WBCS 3000) electrochemical testing equipment. The cells were cycled using a constant current of 43.5 mA g^{-1} at a voltage range of between 3.0 and 4.3 V.

3. Results and Discussions

The most obvious advantage of using this combustion route is the ease of the method and speed of the reaction which is over in a few seconds. The precursors are already in dry form, and, subsequently, the thermal annealing can be done directly without further drying or precalcination process. Therefore, the synthesis method has the advantage of producing homogeneous materials with the resulting final products free from impurities, even for the Ni-rich stoichiometries. Thus, a whole range of solid solutions of $\text{LiCo}_{1-x}\text{Ni}_x\text{O}_2$ ($x = 0, 0.1, \dots, 0.9$) materials are obtainable as pure, single-phase compounds. So far, no researchers have shown that all the solid solutions of $\text{LiCo}_{1-x}\text{Ni}_x\text{O}_2$ ($x = 0, 0.1, \dots, 0.9$) materials in pure form are obtainable by using one synthesis method. For example, Ohzuku et al. [12], Makimura and Ohzuku [13], Julien et al. [14], Saadoune and Delmas [15], Nayoze et al. [16], all show only one stoichiometry with their respective synthesis methods. The others produce $\text{LiCo}_{1-x}\text{Ni}_x\text{O}_2$ materials that are not pure,

containing minor phases [17], or materials that do not show good layered structures [18].

The XRD patterns of the $\text{LiCo}_{1-x}\text{Ni}_x\text{O}_2$ ($x = 0, 0.1, \dots, 0.9$) materials are shown in Figure 1. They are taken with high counts in order to show that there are no minor phases and impurity peaks present in the samples. The samples are all pure, layered compounds. This means that the Ni-ions have been successfully substituted in the LiCoO_2 structure. It can be clearly observed that all of the fingerprint peaks, namely, (003), (101), (006), (012), (104), (018), and (110) are easily identifiable in all of the XRD patterns. All the diffraction peaks can be indexed with α - NaFeO_2 -type structure based on the hexagonal crystal system with $R\bar{3}m$ space group. They are isostructural with LiNiO_2 and LiCoO_2 phases as compared with the XRD patterns in the ICDD database corresponding to patterns number 98-000-9674 and 98-001-1288, respectively. The XRD patterns also show sharp peaks in the spectra indicating a high degree of crystallinity of the materials. Clear peak splittings of the (006)/(012) and the (008)/(110) doublets are an indication of highly layered structure [19, 20]. It is observed in our samples that the (006)/(012) and the (008)/(110) peak splittings are more distinct in the lesser Ni content materials of the $\text{LiCo}_{1-x}\text{Ni}_x\text{O}_2$ which are an indication that high nickel content reduces the layered characteristics of the compounds. The reference intensity ratio (RIR) and R factor are given by the following expressions:

$$\begin{aligned} \text{RIR} &= \frac{I_{(003)}}{I_{(104)}}, \\ R &= \frac{I_{(006)} + I_{(012)}}{I_{(101)}}, \end{aligned} \quad (1)$$

and they are taken as a measure of the cation ordering of the materials [17, 21]. A high RIR of 1.2 and above indicates good cation ordering [21]. As for the R factor, values of less than 1.0 indicate good cation ordering [18, 22]. Our data indicates high RIR values of above 1.2 and very low R factor values for the materials $x = 0.1$ to 0.5 of the $\text{LiCo}_{1-x}\text{Ni}_x\text{O}_2$ cathode materials corresponding to the respective compounds to reveal the splitting of the (006)/(012) peaks. Ionic radius plays an important role in the cation mixing phenomenon [17]. The Li^+ , Co^{3+} , Ni^{3+} , and Ni^{2+} ionic radii are 0.76 Å, 0.55 Å, 0.56 Å, and 0.69 Å (in coordination 6), respectively [23]. It can be seen that the Ni^{2+} ion is quite similar in size to the Li^+ ion; therefore, cation mixing between these two ions is more likely especially in the high Ni content materials. There is also more likelihood of Ni to exist in the Ni^{2+} oxidation state for the Ni-rich samples. Our results indicate that for $x \leq 0.5$ in the $\text{LiCo}_{1-x}\text{Ni}_x\text{O}_2$ materials, the cation ordering is very good, and these materials are expected to perform well in the electrochemical tests.

Cyclic voltammograms of the $\text{LiCo}_{1-x}\text{Ni}_x\text{O}_2$ materials are shown in Figure 2. The oxidation peaks seem to increase as the Ni content increases in the materials. The oxidation and reduction peaks are listed in Table 1. There seem to be two broad reduction peaks in the Ni-substituted materials compared to those of the pure LiCoO_2 material. This is

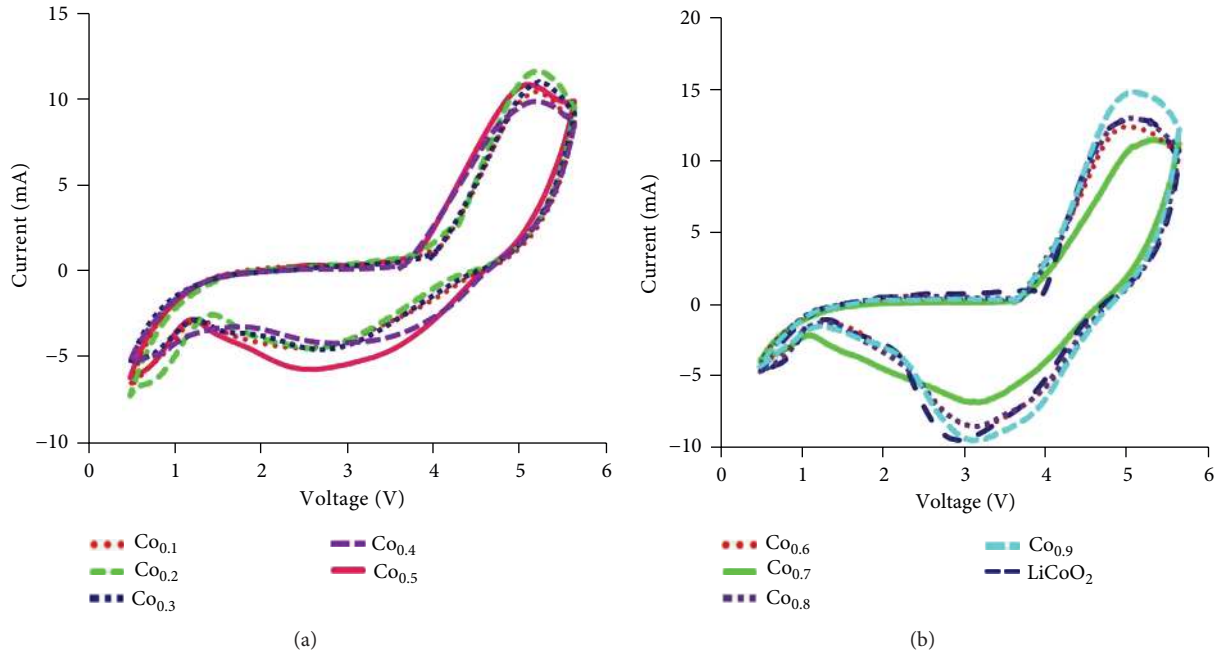


FIGURE 2: Cyclic voltammogram of (a) $\text{LiCo}_{1-x}\text{Ni}_x\text{O}_2$ ($x = 0.9$ to 0.5) and (b) $\text{LiCo}_{1-x}\text{Ni}_x\text{O}_2$ ($x = 0.4$ to 0) in voltage range 0.5 to 5.6 V at a scan rate of 3 mVs^{-1} .

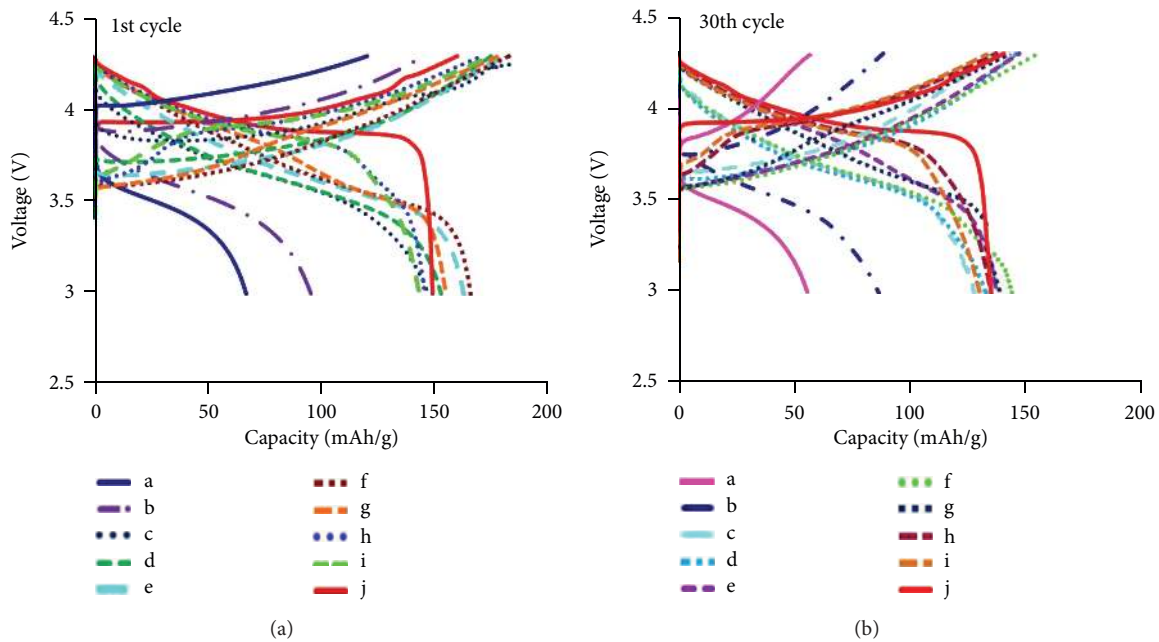


FIGURE 3: Charge-discharge capacities of 1st and 30th cycles of (a) $\text{LiCo}_{0.1}\text{Ni}_{0.9}\text{O}_2$, (b) $\text{LiCo}_{0.2}\text{Ni}_{0.8}\text{O}_2$, (c) $\text{LiCo}_{0.3}\text{Ni}_{0.7}\text{O}_2$, (d) $\text{LiCo}_{0.4}\text{Ni}_{0.6}\text{O}_2$, (e) $\text{LiNi}_{0.5}\text{Co}_{0.5}\text{O}_2$, (f) $\text{LiCo}_{0.6}\text{Ni}_{0.4}\text{O}_2$, (g) $\text{LiCo}_{0.7}\text{Ni}_{0.3}\text{O}_2$, (h) $\text{LiCo}_{0.8}\text{Ni}_{0.2}\text{O}_2$, (i) $\text{LiCo}_{0.9}\text{Ni}_{0.1}\text{O}_2$, and (j) LiCoO_2 .

attributed to the redox couples $\text{Ni}^{4+}/\text{Ni}^{3+}$ and $\text{Ni}^{3+}/\text{Ni}^{2+}$ [24] and is reflected by the double or triple plateaus of the charge-discharge curves of the heavier Ni content materials in Figure 3. It is believed that the Ni-rich materials have both Ni^{3+} and Ni^{2+} ions. The lower voltage plateaus are attributed to the $\text{Ni}^{3+}/\text{Ni}^{2+}$ redox couple. One consequence for the existence of Ni^{2+} ions in the sample is that there

will be the existence of Co^{4+} in the sample to balance the charge. The existence of Co^{4+} is detrimental to the electrochemical performance of the materials because Co^{4+} is not electroactive. This may be one of the reasons why the heavier Ni content samples, $\text{LiCo}_{1-x}\text{Ni}_x\text{O}_2$ ($x = 0.9$ to 0.8), do not show good electrochemical charge-discharge as seen later.

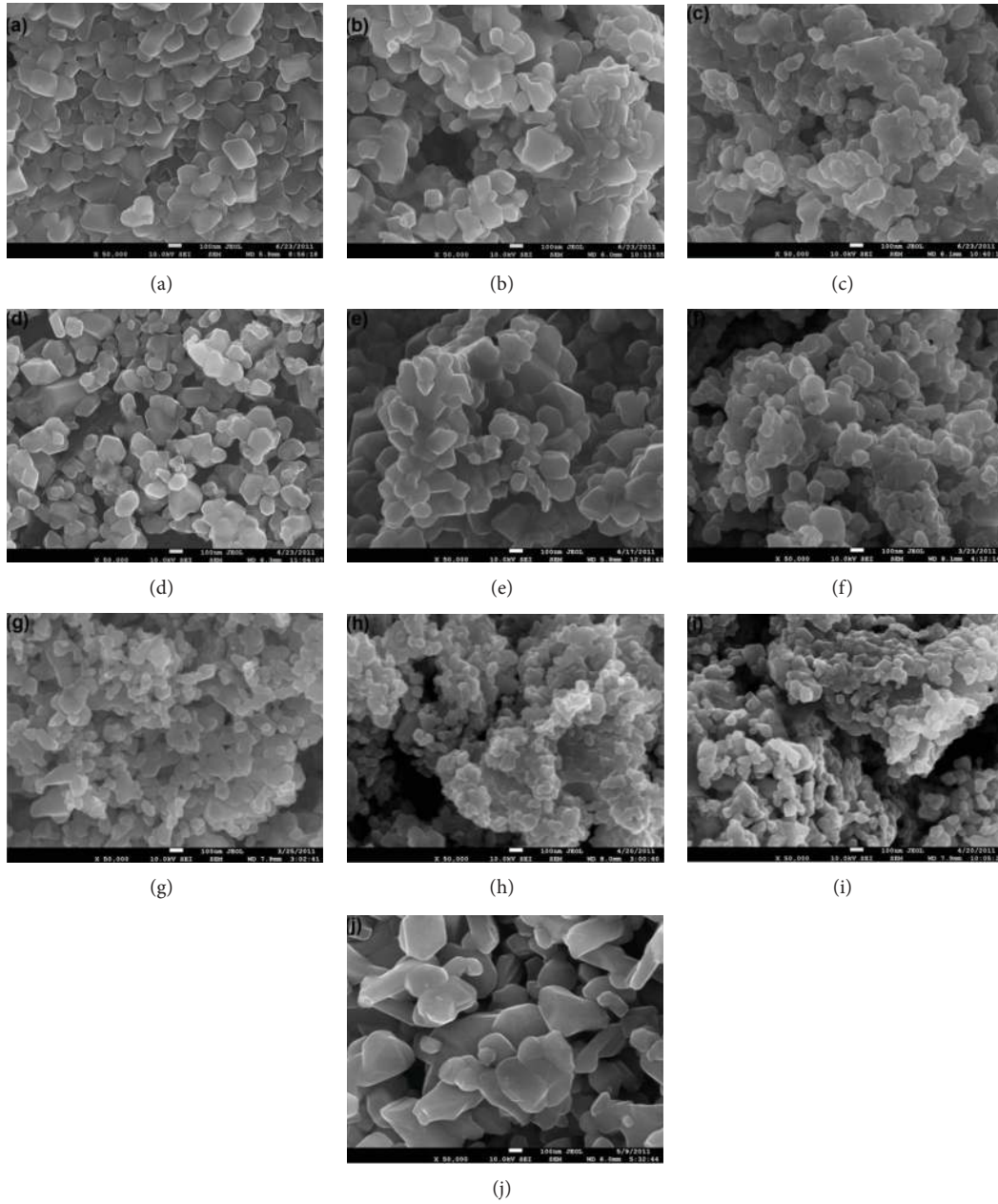


FIGURE 4: SEM images of (a) $\text{LiCo}_{0.1}\text{Ni}_{0.9}\text{O}_2$, (b) $\text{LiCo}_{0.2}\text{Ni}_{0.8}\text{O}_2$, (c) $\text{LiCo}_{0.3}\text{Ni}_{0.7}\text{O}_2$, (d) $\text{LiCo}_{0.4}\text{Ni}_{0.6}\text{O}_2$, (e) $\text{LiNi}_{0.5}\text{Co}_{0.5}\text{O}_2$, (f) $\text{LiCo}_{0.6}\text{Ni}_{0.4}\text{O}_2$, (g) $\text{LiCo}_{0.7}\text{Ni}_{0.3}\text{O}_2$, (h) $\text{LiCo}_{0.8}\text{Ni}_{0.2}\text{O}_2$, (i) $\text{LiCo}_{0.9}\text{Ni}_{0.1}\text{O}_2$, and (j) LiCoO_2 .

The first cycle and thirtieth cycle charge-discharge curves of the materials are shown in Figure 3. It can be seen that *via* this synthesis route, LiCoO_2 shows a specific capacity of 149 mAh g^{-1} which is better than the commercial value of about 120 mAh g^{-1} .

As was discussed earlier, the combustion synthesis results in highly ordered layered compounds that show good electrochemical performance. The discharge profile of the LiCoO_2 material exhibiting a flat plateau at a high average voltage of about 3.9 V illustrates why LiCoO_2 is a very popular commercial cathode material hard to match by other cathode materials. Four of the materials, $\text{LiCo}_{0.4}\text{Ni}_{0.6}\text{O}_2$, $\text{LiCo}_{0.5}\text{Ni}_{0.5}\text{O}_2$,

$\text{LiCo}_{0.6}\text{Ni}_{0.4}\text{O}_2$, and $\text{LiCo}_{0.7}\text{Ni}_{0.3}\text{O}_2$, all show better initial capacities than LiCoO_2 . The stoichiometry of $\text{LiCo}_{0.6}\text{Ni}_{0.4}\text{O}_2$ shows the best specific capacity of 165 mAh g^{-1} over the voltage range of 4.3 to 3.0 V in the first cycle. The voltage plateau, however, is lower than that of LiCoO_2 and slopping down more drastically to 3.0 V. This means that the energy density of the material is slightly lowered due to the lower voltage plateau. This material also suffers from the most capacity loss at the 30th cycle (16.3%) as given in Table 1. LiCoO_2 , on the other hand, only lost 9.5% capacity at the 30th cycle. Another material that seems to show good performance with higher average voltage than $\text{LiCo}_{0.6}\text{Ni}_{0.4}\text{O}_2$ is $\text{LiCo}_{0.7}\text{Ni}_{0.3}\text{O}_2$.

TABLE 1: Electrochemical performances of $\text{LiCo}_{1-x}\text{Ni}_x\text{O}_2$ ($x = 0, 0.1, \dots, 0.9$) and LiCoO_2 annealed at 700°C for 24 h.

Material 700°C, 24 h	Theoretical value	1st discharge capacity (mAh g ⁻¹)	2nd discharge capacity (mAh g ⁻¹)	30th discharge capacity (mAh g ⁻¹)	Capacity loss after 30th cycles (%)	Oxidation peak (V)	Reduction peak (V)	RIR $I_{(003)}/I_{(104)}$	R factor $[I_{(006)} + I_{(012)}]/I_{(101)}$
$\text{LiCo}_{0.1}\text{Ni}_{0.9}\text{O}_2$	274.43	66	61	56	15.15	5.18	2.80	0.94	1.00
$\text{LiCo}_{0.2}\text{Ni}_{0.8}\text{O}_2$	274.36	95	90	86	9.47	5.11	2.76	1.07	0.83
$\text{LiCo}_{0.3}\text{Ni}_{0.7}\text{O}_2$	274.35	146	141	113	22.6	5.15	2.82	1.17	0.62
$\text{LiCo}_{0.4}\text{Ni}_{0.6}\text{O}_2$	274.23	152	150	132	13.16	5.10	2.92	1.32	0.62
$\text{LiCo}_{0.5}\text{Ni}_{0.5}\text{O}_2$	274.16	162	158	136	16.05	4.99	2.63	1.33	0.54
$\text{LiCo}_{0.6}\text{Ni}_{0.4}\text{O}_2$	274.10	165	162	138	16.36	4.89	3.22	1.38	0.51
$\text{LiCo}_{0.7}\text{Ni}_{0.3}\text{O}_2$	274.03	155	150	138	10.97	4.65	3.35	1.40	0.53
$\text{LiCo}_{0.8}\text{Ni}_{0.2}\text{O}_2$	273.96	145	140	134	6.94	4.92	3.14	1.42	0.49
$\text{LiCo}_{0.9}\text{Ni}_{0.1}\text{O}_2$	273.89	143	138	129	9.79	4.99	3.12	1.46	0.43
LiCoO_2	273.83	149	146	134	9.46	5.04	2.95	1.58	0.43

This material shows specific capacity of 155 mAh g^{-1} and 138 mAh g^{-1} for the 1st and 30th cycles, respectively. At the 30th cycle, $\text{LiCo}_{0.3}\text{Ni}_{0.7}\text{O}_2$ seems to perform better than $\text{LiCo}_{0.6}\text{Ni}_{0.4}\text{O}_2$ with only about 11% lost in capacity. The discharge plateau is also quite similar to that of LiCoO_2 . The good performance of the materials is believed to be attributable to several factors such as those of highly ordered crystal structure and smaller particle size as discussed later.

The SEM images of LiCoO_2 and $\text{LiCo}_{1-x}\text{Ni}_x\text{O}_2$ ($x = 0, 0.1, \dots, 0.9$) are displayed in Figure 4. The images show that all samples are well-formed polycrystalline materials. The images show that the introduction of Ni in the LiCoO_2 lattice immediately decreases the crystallite size of the $\text{LiCo}_{1-x}\text{Ni}_x\text{O}_2$ materials. The crystal size of LiCoO_2 seem larger compared to the Ni-substituted materials. All the materials have mostly polyhedral-type crystals. Samples (a), (b), and (c) have larger crystallite sizes of about 50 to 300 nm but smaller than LiCoO_2 crystallite size which is about a few microns in size. Samples (d), (e), and (f) have very similar crystallite size of about 50 to 200 nm which are bigger than those of samples (g), (h), and (i). Samples (g), (h), and (i) have the smallest range of crystallite sizes of about 50 to 100 nm. Some of the crystals seem to aggregate slightly into larger particles. It is clear here that the smaller crystallite size of nm range of the samples, $\text{LiCo}_{0.7}\text{Ni}_{0.3}\text{O}_2$, $\text{LiCo}_{0.8}\text{Ni}_{0.2}\text{O}_2$, and $\text{LiCo}_{0.9}\text{Ni}_{0.1}\text{O}_2$, contributes to better performance in terms of specific capacity as well as capacity retention of the materials [25]. The high surface area to volume ratio of nanocrystals increased the efficiency of the electrochemical process which is a surface-dependent phenomenon.

4. Conclusion

$\text{LiCo}_{1-x}\text{Ni}_x\text{O}_2$ ($x = 0, 0.1, \dots, 0.9$) materials, via the self propagating combustion method, have been successfully synthesized and show single-phase, pure products with high crystallinity. The $\text{LiCo}_{1-x}\text{Ni}_x\text{O}_2$ ($x = 0.1, \dots, 0.5$) materials show good cation ordering and exhibit high specific capacities with slightly lower and slopping discharge plateaus. In

conclusion, the self-propagating combustion synthesis is a good synthesis method for getting well-ordered structures of $\text{LiCo}_{1-x}\text{Ni}_x\text{O}_2$ materials with electrochemical performance comparable to LiCoO_2 .

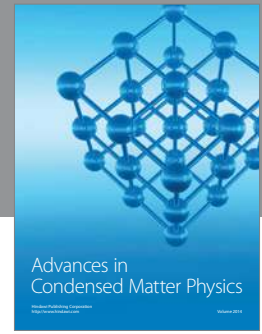
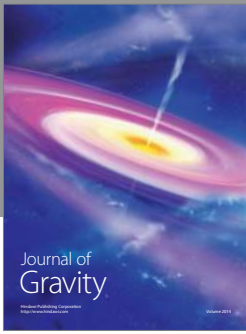
Acknowledgments

The authors would like to thank the Institute of Science, UiTM, Shah Alam, Malaysia, for funding of the project and also the Academy of Science, Malaysia, for the research Grant no. P.20c.

References

- [1] M. Y. Song, I. Kwon, H. Kim, S. Shim, and D. R. Mumm, "Synthesis of LiNiO_2 cathode by the combustion method," *Journal of Applied Electrochemistry*, vol. 36, no. 7, pp. 801–805, 2006.
- [2] V. Subramanian and G. T. K. Fey, "Preparation and characterization of $\text{LiNi}_{0.7}\text{Co}_{0.2}\text{Ti}_{0.05}\text{M}_{0.05}\text{O}_2$ ($M = \text{Mg, Al and Zn}$) systems as cathode materials for lithium batteries," *Solid State Ionics*, vol. 148, no. 3-4, pp. 351–358, 2002.
- [3] T. Ohzuku and R. J. Brodd, "An overview of positive-electrode materials for advanced lithium-ion batteries," *Journal of Power Sources*, vol. 174, no. 2, pp. 449–456, 2007.
- [4] S. Castro-García, C. Julien, M. A. Sefiaris-Rodríguez, and D. Mazás-Brandariz, "Influence of the synthesis method on the structural and electrochemical properties of $\text{LiCo}_{1-y}\text{Ni}_y\text{O}_2$ oxides," *Ionics*, vol. 6, no. 5-6, pp. 434–440, 2000.
- [5] P. Periasamy, H. S. Kim, S. H. Na, S. I. Moon, and J. C. Lee, "Synthesis and characterization of $\text{LiNi}_{0.8}\text{Co}_{0.2}\text{O}_2$ prepared by a combustion solution method for lithium batteries," *Journal of Power Sources*, vol. 132, no. 1-2, pp. 213–218, 2004.
- [6] A. K. Arof, "Characteristics of LiMO_2 ($M = \text{Co, Ni, Ni}_{0.2}\text{Co}_{0.8}, \text{Ni}_{0.8}\text{Co}_{0.2}$) powders prepared from solution of their acetates," *Journal of Alloys and Compounds*, vol. 449, no. 1-2, pp. 288–291, 2008.
- [7] E. Y. Bang, D. R. Mumm, H. R. Park, and M. Y. Song, "Lithium nickel cobalt oxides synthesized from Li_2CO_3 , NiO and Co_3O_4 by the solid-state reaction method," *Ceramics International*, vol. 38, pp. 3635–3641, 2012.

- [8] Y. D. Zhong, X. B. Zhao, G. S. Cao, J. P. Tu, and T. J. Zhu, "Characterization of particulate sol-gel synthesis of $\text{LiNi}_{0.8}\text{Co}_{0.2}\text{O}_2$ via maleic acid assistance with different solvents," *Journal of Alloys and Compounds*, vol. 420, no. 1-2, pp. 298–305, 2006.
- [9] J. Xie, X. Huang, J. Dai, Z. Zhu, Y. Zheng, and Z. Liu, "Hydrothermal synthesis of $\text{LiNi}_{0.9}\text{Co}_{0.1}\text{O}_2$ cathode materials," *Ceramics International*, vol. 36, no. 8, pp. 2489–2492, 2010.
- [10] C.-H. Lu and H.-C. Wang, "Preparation and electrochemical characteristics of microemulsion-derived $\text{Li}(\text{Ni}, \text{Co})\text{O}_2$ nanopowders," *Journal of Materials Science*, vol. 42, no. 3, pp. 752–758, 2007.
- [11] N. Kamarulzaman, R. H. Y. Subban, K. Ismail et al., "Characterization and microstructural studies of LiFe_2O_8 synthesized by the self propagating high temperature combustion method," *Ionics*, vol. 11, no. 5-6, pp. 446–450, 2005.
- [12] T. Ohzuku, K. Nakura, and T. Aoki, "Comparative study of solid-state redox reactions of $\text{LiCo}_{1/4}\text{Ni}_{3/4}\text{O}_2$ and $\text{LiAl}_{1/4}\text{Ni}_{3/4}\text{O}_2$ for lithium-ion batteries," *Electrochimica Acta*, vol. 45, no. 1-2, pp. 151–160, 1999.
- [13] Y. Makimura and T. Ohzuku, "Lithium insertion material of $\text{LiNi}_{1/2}\text{Mn}_{1/2}\text{O}_2$ for advanced lithium-ion batteries," *Journal of Power Sources*, vol. 119–121, pp. 156–160, 2003.
- [14] C. Julien, M. A. Camacho-Lopez, T. Mohan, S. Chitra, P. Kalyani, and S. Gopukumar, "Combustion synthesis and characterization of substituted lithium cobalt oxides in lithium batteries," *Solid State Ionics*, vol. 135, no. 1–4, pp. 241–248, 2000.
- [15] I. Saadoun and C. Delmas, "On the $\text{Li}_x\text{Ni}_{0.8}\text{Co}_{0.2}\text{O}_2$ System," *Journal of Solid State Chemistry*, vol. 136, no. 1, pp. 8–15, 1998.
- [16] C. Nayoze, F. Ansart, C. Laberty, J. Sarrias, and A. Rousset, "New synthesis method of $\text{LiM}_{1-x}\text{M}'_x\text{O}_2$ elaborated by soft chemistry for rechargeable batteries (M and M' = Ni, Co or Mn)," *Journal of Power Sources*, vol. 99, no. 1-2, pp. 54–59, 2001.
- [17] J. N. Reimers, E. Rossen, C. D. Jones, and J. R. Dahn, "Structure and electrochemistry of $\text{Li}_x\text{Fe}_y\text{Ni}_{1-y}\text{O}_2$," *Solid State Ionics*, vol. 61, no. 4, pp. 335–344, 1993.
- [18] G. Ting-Kuo Fey, V. Subramanian, and J. G. Chen, "Synthesis of non-stoichiometric lithium nickel cobalt oxides and their structural and electrochemical characterization," *Electrochemistry Communications*, vol. 3, no. 5, pp. 234–238, 2001.
- [19] X.-M. Liu, W.-L. Gao, and B.-M. Ji, "Synthesis of $\text{LiNi}_{1/3}\text{Co}_{1/3}\text{Mn}_{1/3}\text{O}_2$ nanoparticles by modified Pechini method and their enhanced rate capability," *Journal of Sol-Gel Science and Technology*, vol. 61, no. 1, pp. 56–61, 2012.
- [20] J. R. Dahn, "Structure and electrochemistry of $\text{Li}_{1-y}\text{NiO}_2$ and a new Li_2NiO_2 phase with the $\text{Ni}(\text{OH})_2$ structure," *Solid State Ionics*, vol. 44, no. 1-2, pp. 87–97, 1990.
- [21] S. Yang, X. Wang, X. Yang et al., "Influence of Li source on tap density and high rate cycling performance of spherical $\text{Li}[\text{Ni}_{1/3}\text{Co}_{1/3}\text{Mn}_{1/3}]\text{O}_2$ for advanced lithium-ion batteries," *Journal of Solid State Electrochemistry*, vol. 16, no. 3, pp. 1229–1237, 2012.
- [22] S. H. Park, K. S. Park, Y. Sun Kook, K. S. Nahm, Y. S. Lee, and M. Yoshio, "Structural and electrochemical characterization of lithium excess and Al-doped nickel oxides synthesized by the sol-gel method," *Electrochimica Acta*, vol. 46, no. 8, pp. 1215–1222, 2001.
- [23] D. R. Lide, *Handbook of Chemistry and Physics*, CRC Press, Boca Raton, Fla, USA, 1995.
- [24] R. Santhanam and B. Rambabu, "Improved high rate cycling of Li-rich $\text{Li}_{1.10}\text{Ni}_{1/3}\text{Co}_{1/3}\text{Mn}_{1/3}\text{O}_2$ cathode for lithium batteries," *International Journal of Electrochemical Science*, vol. 4, no. 12, pp. 1770–1778, 2009.
- [25] K. Ozawa, *Lithium-Ion Rechargeable Batteries*, Wiley-VCH, New York, NY, USA, 2009.



Hindawi

Submit your manuscripts at
<http://www.hindawi.com>

